AIMS Mathematics

http://www.aimspress.com/journal/Math

AIMS Mathematics, 8(4): 9009–9026.
DOI: 10.3934/math.2023451
Received: 22 December 2022
Revised: 29 January 2023
Accepted: 02 February 2023
Published: 10 February 2023

Research article

Barycentric rational collocation method for fractional reaction-diffusion equation

Jin Li*

School of Science, Shandong Jianzhu University, Jinan, 250101, China

* **Correspondence:** Email: lijin@lsec.cc.ac.cn; Tel: 18615186091.

Abstract: Barycentric rational collocation method (BRCM) for solving spatial fractional reaction-diffusion equation (SFRDE) is presented. New Gauss quadrature with weight function $(s_\theta - \tau)^{\xi-\alpha}$ is constructed to approximate fractional integral. Matrix equation of SFRDF is obtained from discrete SFRDE. With help of the error of barycentrix rational interpolation, convergence rate is obtained.

Keywords: linear barycentric rational interpolation; collocation method; fractional reaction-diffusion equation
Mathematics Subject Classification: 65D32, 65D30, 65R20

1. Introduction

Consider the spatial fractional reaction-diffusion equation (SFRDE)

$$\frac{\partial u}{\partial t} - {}_0^C D_s^\alpha u(s,t) = f(s,t), \quad (s,t) \in (a,b) \times (0,T), \tag{1.1}$$

$$u(s,0) = \phi(s), \quad s \in (a,b), \tag{1.2}$$

where $\alpha \in (1,2)$ and

$${}_0^C D_s^\alpha u(s,t) = \begin{cases} \dfrac{1}{\Gamma(\xi-\alpha)} \displaystyle\int_0^s \frac{\partial^\xi u(\tau,t)}{\partial \tau^\xi} \frac{d\tau}{(s-\tau)^{\alpha+1-\xi}}, & n-1 \le \xi \le n, \\ u^{(n)}(s_0), & n \in N, \end{cases} \tag{1.3}$$

where $\Gamma(\alpha) = \int_0^\infty x^{\alpha-1} e^{-x} dx, x \in (0,\infty)$ is Γ function, see [1].

Reaction-diffusion equation (RDE) as

$$\frac{\partial u}{\partial t} - \frac{\partial^2 u}{\partial s^2} = f(s,t), \quad (s,t) \in (a,b) \times (0,T), \tag{1.4}$$

as a kind of important partial differential equation, originates from a wide range of diffusion phenomena, influent flow theory, biochemistry, engineering,brain activity detection [2] and other fields.

Systems of fractional differential equations are also used in the study of electric circuits. In reference [3], explicit solutions for several families of such systems, both homogeneous and inhomogeneous cases, both commensurate and incommensurate are presented. Multi-dimensional time-dependent spatial fractional convection-diffusion (SFCD) equations [4] based on the Riemann-Liouville (RL) derivative is studied by high-efficient accurate mesh-free scheme. Time fractional diffusion equation [5] with discontinuous coefficients is investigated by immersed finite element (IFE) method, stabilities and error estimates are obtained. In reference [6], the authors have developed novel numerical schemes for the Caputo fractional derivative with order $\alpha \in (1, 2)$ by cubic interpolating polynomial and cubic Hermite interpolation. A space-time finite element method for the multi-term time-space fractional diffusion equation is proposed in reference [7], the existence, uniqueness and stability of numerical scheme are also discussed. Weak Galerkin finite element [8] method to solve multi-term time fractional diffusion equation is considered, the stability analysis for both semi-discrete and fully-discrete schemes are presented. Collocation approach [9] is developed and stability of this scheme is investigated.

Barycentrix interpolation collocation [10–15] have been developed rapidly. In the recent paper, heat conduction equation [16], integral-differential equation [17], biharmonic equation [18, 19] and fractional differential equations [20] have been solved by linear barycentrix rational collocation methods (LBRCM). In the paper [21–24], barycentric interpolation collocation method for nonlinear parabolic partial differential equations [25], incompressible plane elastic problems and plane elastic problems [26] and so on are presented.

In this paper, SFRDE is considered by linear barycentrix interpolation collocation methods. The fractional term is calculated by fractional integration which the singular part is changed to Riemman integral under the condition that the density function have one order more regularity. Different from the classical Gauss quadrature, new Gauss quadrature with weight function $(s_\theta - \tau)^{\xi-\alpha}$ is constructed which have high accuracy. Then matrix equation of SFRDF is obtained from discrete SFRDE and convergence rate is proposed.

2. Matrix equation of SFRDE

Matrix equation of SFRDE is given in this part. The domain $[a, b] \times [0, T]$ is divided into

$$(s_i, t_j), i = 0, 1, \cdots, \ m, j = 0, 1, \cdots, n,$$

which can be chosen as equidistant nodes or Chebyshev nodes [27]. For equidistant meshes, we have $h_s = \frac{b-a}{m}, h_t = \frac{T}{n}$.

The barycentric interpolation function is given by

$$u(s, t) := \sum_{i=0}^{m} \sum_{j=0}^{n} R_i(s) R_j(t) u_{ij}, \tag{2.1}$$

where $u_{ij} = u(s_i, t_j)$ and

$$R_i(s) = \frac{\dfrac{w_i}{s - s_i}}{\displaystyle\sum_{k=0}^{m} \frac{w_k}{s - s_k}}, \quad R_j(t) = \frac{\dfrac{\lambda_j}{t - t_j}}{\displaystyle\sum_{k=0}^{n} \frac{\lambda_k}{t - t_k}}, \tag{2.2}$$

is basis function [28]. For different weight function w_i and λ_j, there are different kind of barycentric interpolation, such as barycentric Lagrange interpolation (BLI) and barycentric rational interpolation (BRI) [21] and so on.

The w_i denoted as weight function of BLI is defined as

$$w_i = \frac{1}{\prod\limits_{j=0, j\neq i}^{m} s_i - s_j}, \quad \lambda_k = \frac{1}{\prod\limits_{j=0, j\neq k}^{l} t_k - t_j}, \tag{2.3}$$

λ_j of BRI is defined as

$$\begin{aligned} w_i &= \sum_{r_1 \in J_i} (-1)^{r_1} \prod_{k=r_1, r_1 \neq i}^{r_1 + d_s} \frac{1}{s_i - s_k}, \quad J_i = \{r_1 : i - d_s \leq r_1 \leq i\}, \\ \lambda_k &= \sum_{r_2 \in J_k} (-1)^{r_3} \prod_{i=r_2, r_2 \neq k}^{r_2 + d_t} \frac{1}{t_k - t_i}, \quad J_k = \{r_2 : k - d_t \leq r_2 \leq k\}, \end{aligned} \tag{2.4}$$

where $r_1 \in \{0, 1, \cdots, m - d_s\}$, $r_2 \in \{0, 1, \cdots, n - d_t\}$, the parameters d_s, d_t are integers and $0 \leq d_s \leq m, 0 \leq d_t \leq n$.

As there are singularity in Eq (1.3), the numerical methods can not get high accuracy, so we change (1.3) by fractional integration to overcome the difficulty singularity. We get

$$\begin{aligned} {}_0^C D_s^\alpha u(s,t) &= \frac{1}{\Gamma(\xi - \alpha)} \int_0^x \frac{\partial^\xi u(\tau, t)}{\partial \tau^\xi} \frac{d\tau}{(s - \tau)^{\alpha + 1 - \xi}} \\ &= \frac{1}{\Gamma(\xi - \alpha)(\xi - \alpha)} \left[\frac{\partial^\xi u(0, t)}{\partial s^\xi} s^{\xi - \alpha} + \int_0^s \frac{\partial^{\xi + 1} u(\tau, t)}{\partial \tau^{\xi + 1}} \frac{d\tau}{(s - \tau)^{\alpha - \xi}} \right] \\ &= \Gamma_\alpha^\xi \left[\frac{\partial^\xi u(0, t)}{\partial s^\xi} s^{\xi - \alpha} + \int_0^s \frac{\partial^{\xi + 1} u(\tau, t)}{\partial \tau^{\xi + 1}} \frac{d\tau}{(s - \tau)^{\alpha - \xi}} \right], \end{aligned} \tag{2.5}$$

where

$$\Gamma_\alpha^\xi = \frac{1}{\Gamma(\xi - \alpha)(\xi - \alpha)}.$$

Combining (2.5) and (1.1), we have

$$\frac{\partial u}{\partial t} - \Gamma_\alpha^\xi \left[\frac{\partial^\xi u(0, t)}{\partial s^\xi} s^{\xi - \alpha} + \int_0^s \frac{\partial^{\xi + 1} u(\tau, t)}{\partial \tau^{\xi + 1}} \frac{d\tau}{(s - \tau)^{\alpha - \xi}} \right] = f(s, t). \tag{2.6}$$

Combining Eqs (2.1) and (2.6), then we get

$$
\begin{aligned}
\sum_{i=0}^{m}\sum_{j=0}^{n}\left[R'_j(t)R_i(s)\right]u_{ij} - \Gamma_{\alpha}^{\xi}\sum_{i=0}^{m}\sum_{j=0}^{n}\left[R_j(t)R_i^{(\xi)}(0)s^{\xi-\alpha}\right]u_{ij}& \\
- -\Gamma_{\alpha}^{\xi}\sum_{i=0}^{m}\sum_{j=0}^{n}\left[R_j(t)\int_0^s\frac{R_i^{(\xi+1)}(\tau)}{(s-\tau)^{\alpha-\xi}}d\tau\right]u_{ij}& \\
= f(s,t),&
\end{aligned}
\tag{2.7}
$$

where

$$
R_k(\tau) = \frac{\dfrac{\lambda_k}{\tau-\tau_k}}{\sum\limits_{k=0}^{n}\dfrac{\lambda_k}{\tau-\tau_k}},
$$

and

$$
\begin{cases}
R_i^{'}(\tau) = R_i(\tau)\left[-\dfrac{1}{\tau-\tau_k} + \dfrac{\sum\limits_{s=0}^{l}\dfrac{\lambda_k}{(\tau-\tau_k)^2}}{\sum\limits_{s=0}^{l}\dfrac{\lambda_k}{\tau-\tau_k}}\right], \\
\qquad\vdots \\
R_i^{(\xi+1)}(\tau) = [R_i^{(\xi)}(\tau)]^{'}, \xi\in\mathbf{N}^+.
\end{cases}
$$

Let $s = s_\mu,\ t = t_\theta$, we get

$$
\begin{aligned}
\sum_{i=0}^{m}\sum_{j=0}^{n}\left[R'_j(t_\theta)R_i(s_\mu)\right]u_{ij} - \Gamma_{\alpha}^{\xi}\sum_{i=0}^{m}\sum_{j=0}^{n}\left[R_j(t_\theta)R_i^{(\xi)}(0)s_\mu^{\xi-\alpha}\right]u_{ij}& \\
- \Gamma_{\alpha}^{\xi}\sum_{i=0}^{m}\sum_{j=0}^{n}\left[R_j(t_\theta)\int_0^{s_\mu}\frac{R_i^{(\xi+1)}(\tau)}{(s_\mu-\tau)^{\alpha-\xi}}d\tau\right]u_{ij}& \\
= f(s_\mu,t_\theta),&
\end{aligned}
\tag{2.8}
$$

where $\mu = 0,1,\cdots,\ m, \theta = 0,1,\cdots,n$.

The integral term of (2.8) can be written as

$$
\int_0^{s_\mu} R_i^{(\xi+1)}(\tau)(s_\mu-\tau)^{\xi-\alpha}d\tau = Q_i(s_\mu) = Q_{i\mu}, \tag{2.9}
$$

then we get

$$
\sum_{i=0}^{m}\sum_{j=0}^{n}\left[R'_j(t_\theta)R_i(s_\mu)\right]u_{ij} - \Gamma_{\alpha}^{\xi}\sum_{i=0}^{m}\sum_{j=0}^{n}\left[R_j(t_\theta)R_i^{(\xi)}(0)s_\mu^{\xi-\alpha} + R_j(t_\theta)Q_i(s_\mu)\right]u_{ij} = f(s_\mu,t_\theta), \tag{2.10}
$$

noting the notation,

$$
R_i(s_\mu) = \delta_{i\mu},\ \ R'_j(t_\theta) = M_{j\theta}^{(01)},\ \ R_j(t_\theta) = \delta_{j\theta},\ \ R_i^{(\xi)}(0) = M_{i\mu}^{(\xi 0)},
$$

where $M_{j\theta}^{(01)}, M_{i\mu}^{(\xi 0)}$ is the first order derivative of barycentrix matrix related with t and s [20].

The integral (2.9) is calculated by

$$Q_{i\mu} = Q_i(s_\mu) = \int_0^{s_\mu} R_i^{(\xi+1)}(\tau)(s_\mu - \tau)^{\xi-\alpha} d\tau := \sum_{i=1}^{g} R_i^{(\xi+1)}(\tau_i^{\theta,\alpha}) G_i^{\theta,\alpha}, \tag{2.11}$$

where $G_i^{\theta,\alpha}$ is Gauss weight and $\tau_i^{\theta,\alpha}$ is Gauss points with weights $(s_\mu - \tau)^{\xi-\alpha}$ [20].

Equation systems (2.10) can be written as

$$\left[I_{m+1} \otimes M^{(01)} - \Gamma_\alpha^\xi \left(T^{\xi,\alpha}\left(I_{n+1} \otimes M_1^{(\xi 0)}\right) + I_{n+1} \otimes Q\right)\right] \begin{bmatrix} u_{00} \\ \vdots \\ u_{0n} \\ u_{10} \\ \vdots \\ u_{1n} \\ u_{m0} \\ \vdots \\ u_{mn} \end{bmatrix} = \begin{bmatrix} f_{00} \\ \vdots \\ f_{0n} \\ f_{10} \\ \vdots \\ f_{nn} \\ f_{m0} \\ \vdots \\ f_{mn} \end{bmatrix}, \tag{2.12}$$

I_{m+1} and I_{n+1} are identity matrices, $\otimes$ is Kronecker product (see [21]),

$$M^{(01)} = [M_{ij}^{(01)}]_{n+1,n+1}, \quad M^{(\xi 0)} = [M_{ij}^{(\xi 0)}]_{n+1,n+1}, \quad Q = [Q_{ij}]_{m+1,m+1},$$

and

$$T^{\xi,\alpha} = diag(s_\mu^{\xi-\alpha}).$$

Then Eq (2.12) can be noted as

$$\left[I_{m+1} \otimes M^{(01)} - \Gamma_\alpha^\xi \left(T^{\xi,\alpha}\left(I_{n+1} \otimes M_1^{(\xi 0)}\right) + I_{n+1} \otimes Q\right)\right] U = F, \tag{2.13}$$

and

$$LU = F, \tag{2.14}$$

with

$$L = I_{m+1} \otimes M^{(01)} - \Gamma_\alpha^\xi \left(T^{\xi,\alpha}\left(I_{n+1} \otimes M_1^{(\xi 0)}\right) + I_{n+1} \otimes Q\right),$$

$$U = [u_{00} \cdots u_{0n}, u_{10} \cdots u_{1n}, u_{m0} \cdots u_{mn}]^T,$$

and

$$F = [f_{00} \cdots f_{0n}, f_{10} \cdots f_{1n}, f_{m0} \cdots f_{mn}]^T.$$

The initial and boundary condition can be dealt with the additional methods or replacement methods [21].

3. Convergence and error analysis

In this part, we present the proof convergence rate of LBRCM for SFRDE. Firstly, we define the error function

$$e(s) = u(s) - p_n(s) = (s - s_i) \cdots (s - s_{i+d})\, u[s_i, s_{i+1}, \ldots, s_{i+d}, s], \tag{3.1}$$

and

$$e(s) = \frac{\sum_{i=0}^{n-d} \lambda_i(s)\,(u(s) - p_i(s))}{\sum_{i=0}^{n-d} \lambda_i(s)} = \frac{A(s)}{B(s)} = O(h^{d+1}), \tag{3.2}$$

where$h = (b - a)/m$,

$$p_n(s) = \frac{\sum_{k=0}^{n} \frac{\lambda_i}{s - s_i} u_i}{\sum_{k=0}^{n} \frac{\lambda_k}{s - s_k}},$$

and

$$A(s) := \sum_{i=0}^{n-d} (-1)^i u\,[x_i, \ldots, s_{i+d}, s]\,,$$

$$B(s) := \sum_{i=0}^{n-d} \lambda_i(s), \lambda_i,$$

is defined as (2.3).

In the following, C denotes positive constant different places maybe its value is different.

Lemma 1. *[10] For $e(s)$ defined as (3.1), there holds*

$$\left|e^{(k)}(s)\right| \le C h^{d+1-k}, \quad u \in C^{d+k+2}[a, b], \quad k = 0, 1, \cdots. \tag{3.3}$$

For the SFRDE, we can get the error function as rational interpolation function of $u(s, t)$ is defined as $r_{mn}(s, t)$

$$r_{mn}(s, t) = \frac{\sum_{i=0}^{m+d_s} \sum_{j=0}^{n+d_t} \frac{w_{i,j}}{(s - s_i)\left(t - t_j\right)} u_{i,j}}{\sum_{i=0}^{m+d_s} \sum_{j=0}^{n+d_t} \frac{w_{i,j}}{(s - s_i)\left(t - t_j\right)}}, \tag{3.4}$$

where

$$w_{i,j} = (-1)^{i-d_s+j-d_t} \sum_{k_1 \in J_i} \prod_{h_1=k_1, h_1 \neq j}^{k_1+d_s} \frac{1}{\left|s_i - s_{h_1}\right|} \sum_{k_2 \in J_i} \prod_{h_2=k_2, h_2 \neq j}^{k_2+d_t} \frac{1}{\left|t_j - t_{h_2}\right|}. \tag{3.5}$$

We define $u(s,t)$ to be

$$
\begin{aligned}
e(s,t) :&= u(s,t) - r_{mn}(s,t) \\
&= (s-s_i)\cdots(s-s_{i+d_s})\,u\left[s_i, s_{i+1}, \ldots, s_{i+d_1}, s\right] \\
&\quad + \left(t-t_j\right)\cdots\left(t-t_{j+d_t}\right)u\left[t_j, t_{j+1}, \ldots, t_{j+d_2}, t\right].
\end{aligned} \tag{3.6}
$$

See [28].

With similar analysis of Lemma 1, we have

Lemma 2. *For $e(s,t)$ defined as (3.6) and $\phi(s,t) \in C^{d_s+k_1+2}[a,b] \times C^{d_t+k_2+2}[0,T]$, then we have*

$$
\left|e^{(k_1,k_2)}(s,t)\right| \le C(h_s^{d_s-k_1+1} + h_t^{d_t-k_2+1}), \tag{3.7}
$$

where $k_1, k_2 = 0, 1, \cdots$.

Combining (2.8) and (1.1), we have

$$
\mathcal{L}e(s,t) := e_t(s,t) - \Gamma(\xi)e_s(0,t) - \Gamma(\xi)\int_0^s \frac{e_{\tau\tau\tau}(\tau,t)}{(s-\tau)^{\alpha-\xi}}d\tau - R_f(s,t), \tag{3.8}
$$

where

$$
R_f(s,t) = f(s,t) - f(s_i,\ \ t_j),\ \ i,j = 0,1,2,\cdots,n.
$$

Let $u(s,t)$ to be the solution of (1.1) and $u_{mn}(s,t)$ is the numerical solution, then we have

$$
\mathcal{L}u_{mn}(s_i,t_j) = f(s_i,t_j),\ \ i,j = 0,1,2,\cdots,m,n,
$$

and

$$
\lim_{\substack{m\to\infty \\ n\to\infty}} u_n(s_i,t_j) = u(s,t).
$$

We get the following theorem.

Theorem 1. *Let*

$$
u_{mn}(s,t) : \mathcal{L}u_{mn}(s_i,t_j) = f(s_i,t_j),\ \ u(s,t) \in C^3[a,b]\times[0,T],
$$

and suppose $\mathcal{L}$ be the invertible operator, we have

$$
|u_{mn}(s_i,t_j) - u(s,t)| \le C(h_s^{d_s-1} + h_t^{d_t}).
$$

Proof. Combining the Lemma 1 and Eq (3.8), we have

$$
\begin{aligned}
|\mathcal{L}e(s,t)| &= \left|e_t(s,t) - \Gamma(\xi)e_{ss}(0,t) - \Gamma(\xi)\int_0^s \frac{e_{\tau\tau\tau}(\tau,t)}{(s-\tau)^{\alpha-\xi}}d\tau - R_f(s,t)\right| \\
&\le |e_t(s,t)| + |\Gamma(\xi)e_{ss}(0,t)| + \left|\Gamma(\xi)\int_0^s \frac{e_{\tau\tau\tau}(\tau,t)}{(s-\tau)^{\alpha-\xi}}d\tau\right| + |R_f(s,t)| \\
&\le C(h_s^{d_s+1} + h_t^{d_t}) + C(h_s^{d_s-1} + h_t^{d_t+1}) + C(h_s^{d_s-1} + h_t^{d_t+1}) \\
&\le C(h_s^{d_s-1} + h_t^{d_t}).
\end{aligned} \tag{3.9}
$$

As $\mathcal{L}$ is invertible operator. Then we have

$$
|u_{mn}(s_i,t_j) - u(s,t)| \le C(h_s^{d_s-1} + h_t^{d_t}).
$$

The proof is completed.

4. Numerical examples

Example is presented to valid our theorem.

Example 1. *Consider the SFRDE*

$$\frac{\partial u}{\partial t} - {}_0^C D_s^\alpha u(s,t) = f(s,t), \quad (s,t) \in (0,1) \times (0,T), \tag{4.1}$$

$$u(s,0) = s^3(1-s)^2, \quad s \in (0,1), \tag{4.2}$$

$$u(s,t) = 0, \quad (s,t) \in R \setminus (0,1) \times (0,T), \tag{4.3}$$

and source term is

$$f(s,t) = -e^{-t}(s^3(1-x)^2 + 6\frac{\Gamma(2)}{\Gamma(4-\alpha)}x^{3-\alpha} - 24\frac{\Gamma(3)}{\Gamma(5-\alpha)}x^{4-\alpha} + 20\frac{\Gamma(4)}{\Gamma(6-\alpha)}x^{5-\alpha}).$$

Its exact solution

$$u(s,t) = e^{-t}s^3(1-s)^2.$$

In Table 1, for different $d_s = d_t = 1, 2, \cdots, 8$ with $m = n = 12, \alpha = 1.5$, errors of BRCM with uniform and non uniform partition are presented, we can take the value $d_s = d_t \geq \frac{n}{2}$ to get the high accuracy.

Table 1. Errors of the BRCM for $d_s = d_t$.

$d_s = d_t$	uniform	nonuniform
1	4.6993e-01	7.5345e-02
2	7.2988e-02	2.8702e-02
3	7.9305e-04	3.4180e-05
4	7.9579e-03	5.0769e-04
5	6.8798e-08	5.7736e-11
6	3.9454e-07	1.3449e-12
7	3.3420e-06	1.4611e-13
8	2.0505e-05	7.1919e-13

In Table 2, Lagrange barycentrix collocation method (LBCM) and RBCM are taken, errors show that accuracy of LBCM is higher than RBCM with $m = n = 12$. For RBCM, we take $m = n = 12$ and $d_s = d_t = 7$. In Table 3, errors of BRCM with uniform and non uniform partition for t are presented with $m = n = 12, \alpha = 1.1$. From Table 3, the accuracy of LBCM is higher than RBCM.

Table 2. Errors of LBCM and RBCM $m = n = 12$.

α	1.1	1.3	1.5	1.7	1.9
LBCM	9.5138e-12	2.4257e-12	1.6542e-12	6.4369e-13	9.5138e-12
RBCM	7.0692e-10	1.4440e-10	2.0669e-10	1.0278e-10	6.9905e-12

Table 3. Errors of LBCM and BRCM for t.

	uniform partition		nonuniform partition	
t	LBCM	RBCM	RBCM	LBCM
0.2	8.1691e-13	1.7989e-10	6.9215e-15	6.8522e-16
0.5	1.7290e-13	1.5966e-10	4.3611e-15	3.0786e-16
1	6.9905e-12	1.9534e-10	7.4393e-13	4.5667e-16
2	1.0755e-12	9.5327e-10	9.7622e-11	5.6413e-14
5	1.4066e-09	7.2354e-08	2.5801e-08	3.1917e-10
10	4.4450e-07	3.0357e-06	9.6720e-07	8.0330e-08

In Tables 4–7, errors of equidistant nodes for fractional reaction-diffusion equation with $\alpha = 1.8$, $\alpha = 1.1$ by LBRCM are presented respectively. As our numerical scheme, there are no influence of fractional differential integral. In Tables 4 and 5, for spatial variable, the convergence rate can reach to $O(h_s^{d_s})$. In Tables 6 and 7, for time variable, the convergence rate also can reach $O(h_t^{d_t})$.

Table 4. Errors of equidistant nodes $\alpha = 1.8$, $d_t = 6$.

$m = n$	$d_s = 2$		$d_s = 3$		$d_s = 4$	
8	1.0675e-02		3.3277e-03		2.2951e-10	
12	4.6326e-03	2.0588	8.6592e-04	3.3202	3.9579e-11	4.3349
16	2.5221e-03	2.1135	3.4191e-04	3.2301	4.1461e-09	-
20	1.5765e-03	2.1058	1.6294e-04	3.3215	3.1576e-05	-

Table 5. Errors of equidistant nodes $\alpha = 1.1$, $d_t = 6$.

$m = n$	$d_s = 2$		$d_s = 3$		$d_s = 4$	
8	1.0675e-02		3.3277e-03		2.2951e-10	
12	4.6326e-03	2.0588	8.6592e-04	3.3202	3.9579e-11	4.3349
16	2.5221e-03	2.1135	3.4191e-04	3.2301	4.1461e-09	-
20	1.5765e-03	2.1058	1.6294e-04	3.3215	3.1576e-05	-

Table 6. Errors of equidistant nodes $\alpha = 1.8$, $d_s = 6$.

$m = n$	$d_t = 2$		$d_t = 3$		$d_t = 4$	
8	3.5786e-06		1.1346e-06		2.8635e-08	
12	1.8147e-06	1.6747	3.6189e-07	2.8182	7.6203e-09	3.2649
16	1.0961e-06	1.7526	1.6175e-07	2.7993	9.4889e-09	-
20	1.7494e-06	-	2.1987e-06	-	3.0205e-06	-

Table 7. Errors of equidistant nodes $\alpha = 1.1$, $d_s = 6$.

$m = n$	$d_t = 2$		$d_t = 3$		$d_t = 4$	
8	9.2124e-06		3.0304e-06		1.0333e-07	
12	4.4886e-06	1.7733	9.9503e-07	2.7467	2.2176e-08	3.7954
16	2.2164e-06	2.4528	3.4298e-07	3.7024	2.5502e-08	-
20	2.4477e-06	-	3.0062e-06	-	4.4543e-06	-

In Tables 8–11, errors of Chebychev nodes for SFRDE with $\alpha = 1.8, \alpha = 1.1$ by LBRCM are presented respectively. The convergence rate of LBRCM is similar as the case of equidistant nodes.

Table 8. Errors of non-equidistant nodes $\alpha = 1.8$, $d_t = 6$.

$m = n$	$d_t = 2$		$d_t = 3$		$d_t = 4$	
8	2.6415e-03		6.6688e-04		5.8189e-11	
12	4.5016e-04	4.3641	5.2184e-05	6.2837	3.1597e-12	7.1849
16	1.3558e-04	4.1714	8.5782e-06	6.2762	6.6963e-13	5.3931
20	5.2841e-05	4.2227	2.1155e-06	6.2737	9.7490e-14	8.6356

Table 9. Errors of non-equidistant nodes $\alpha = 1.1$, $d_t = 6$.

$m = n$	$d_s = 2$		$d_s = 3$		$d_s = 4$	
8	3.4071e-03		9.5228e-04		1.5986e-10	
12	7.3160e-04	3.7941	8.2882e-05	6.0213	4.4480e-12	8.8339
16	2.3489e-04	3.9492	1.4075e-05	6.1631	8.3639e-13	5.8089
20	1.2705e-04	2.7540	3.9952e-06	5.6435	2.0594e-12	-

Table 10. Errors of non-equidistant nodes $\alpha = 1.8$, $d_s = 6$.

$m = n$	$d_t = 2$		$d_t = 3$		$d_t = 4$	
8	1.7801e-06		3.4045e-07		6.8588e-09	
12	6.0764e-07	2.6509	9.2108e-08	3.2242	1.6211e-09	3.5575
16	2.5934e-07	2.9596	2.8259e-08	4.1072	4.2633e-10	4.6428
20	1.3001e-07	3.0946	1.1082e-08	4.1950	1.3837e-10	5.0427

Table 11. Errors of non-equidistant nodes $\alpha = 1.1$, $d_s = 6$.

$m = n$	$d_t = 2$		$d_t = 3$		$d_t = 4$	
8	3.8320e-06		7.3600e-07		1.3248e-08	
12	9.6554e-07	3.3997	1.3592e-07	4.1660	2.4590e-09	4.1534
16	3.3325e-07	3.6978	3.4298e-08	4.7864	5.0191e-10	5.5238
20	1.5073e-07	3.5556	1.2913e-08	4.3777	1.6029e-10	5.1154

From Figures 1–5, errors of LBCM with $m = n = 12, \alpha = 1.1, 1.3, 1.5, 1.7, 1.9$ are proposed.

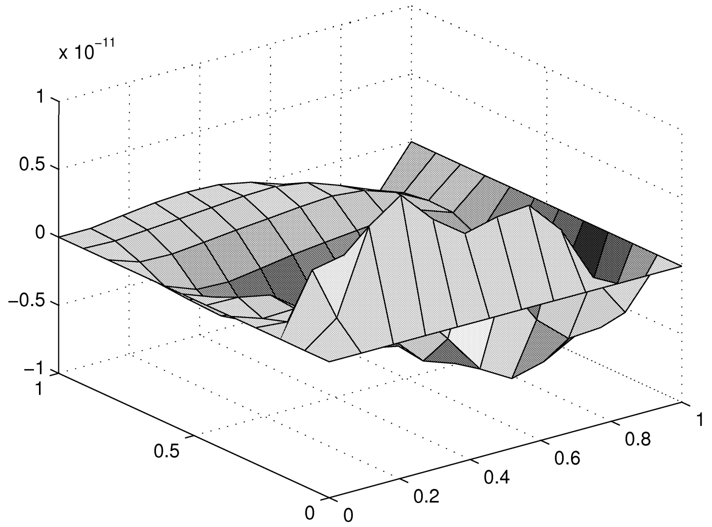

Figure 1. Errors of LBCM with $m = n = 12,\ \alpha = 1.1$.

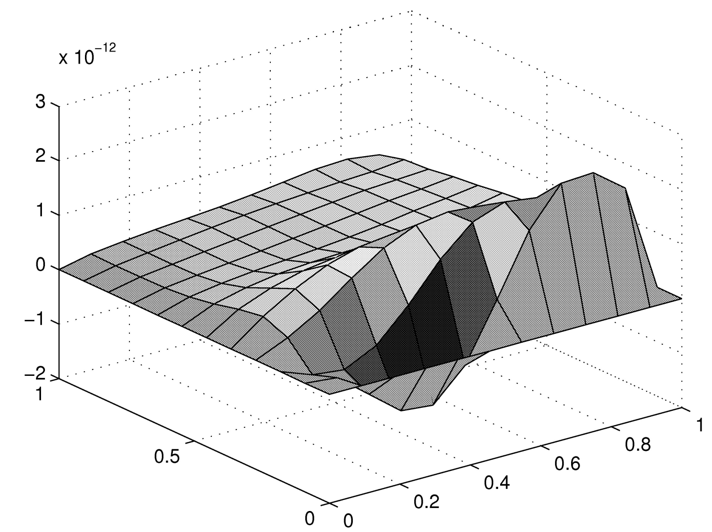

Figure 2. Errors of LBCM with $m = n = 12$, $\alpha = 1.3$.

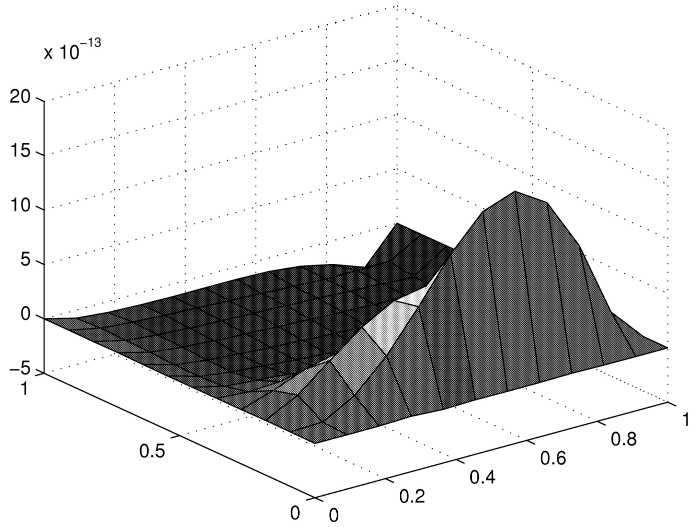

Figure 3. Errors of LBCM with $m = n = 12$, $\alpha = 1.5$.

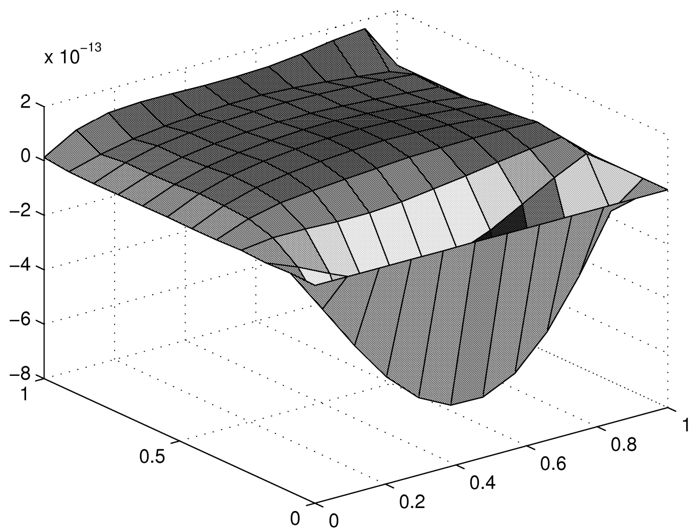

Figure 4. Errors of LBCM with $m = n = 12$, $\alpha = 1.7$.

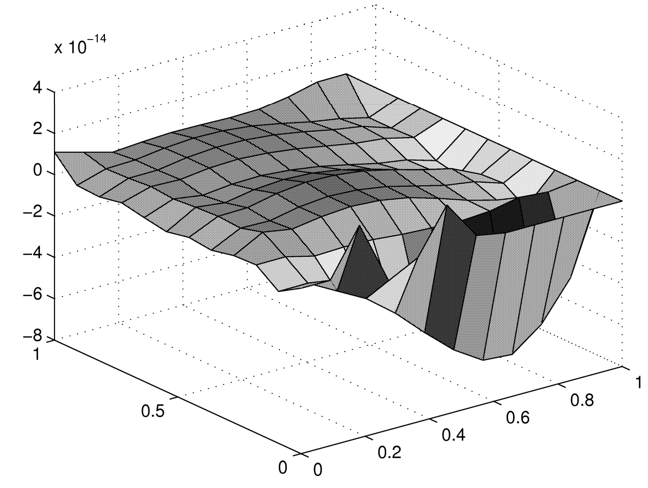

Figure 5. Errors of LBCM with $m = n = 12$, $\alpha = 1.9$.

Figures 6–10, errors of RBCM with $m = n = 12, d_s = d_t = 7, \alpha = 1.1, 1.3, 1.5, 1.7, 1.9$ are proposed. Compared with LBCM and RBCM, the error accuracy can reach 10^{-11} by choosing d_s, d_t approximately.

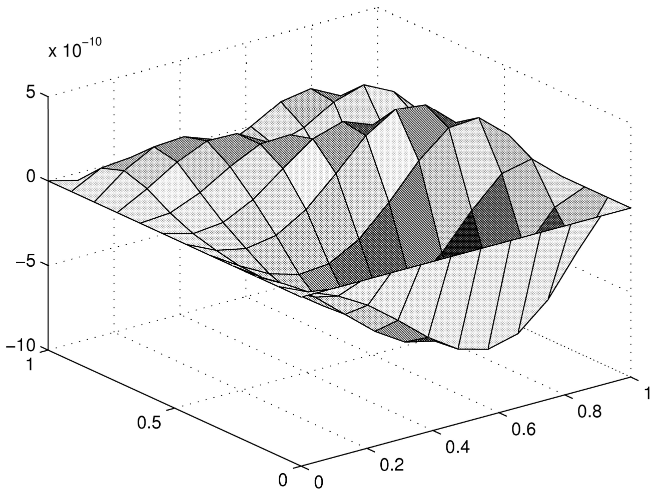

Figure 6. Errors of RBCM with $m = n = 12$, $d_s = d_t = 7$, $\alpha = 1.1$.

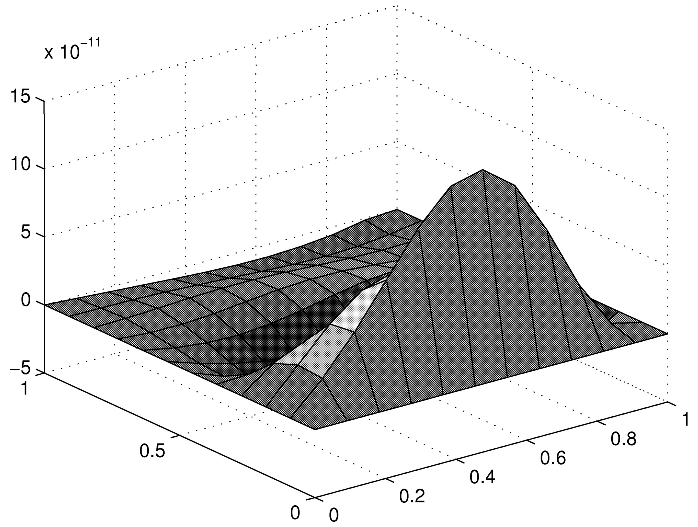

Figure 7. Errors of RBCM with $m = n = 12$, $d_s = d_t = 7$, $\alpha = 1.3$.

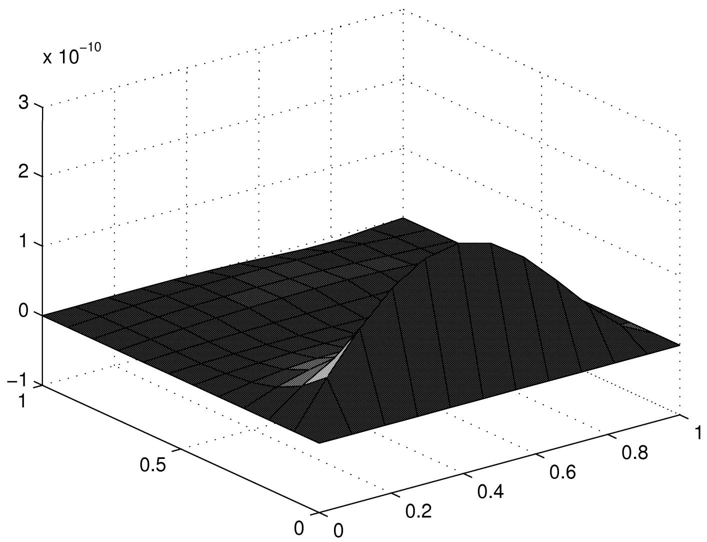

Figure 8. Errors of RBCM with $m = n = 12$, $d_s = d_t = 7$, $\alpha = 1.5$.

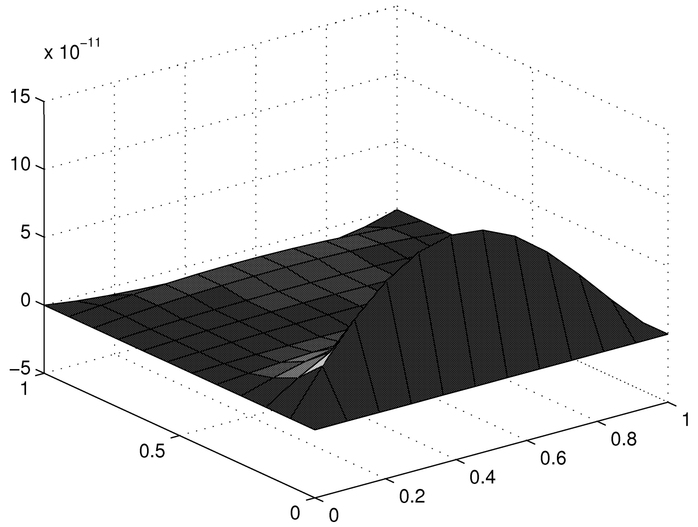

Figure 9. Errors of RBCM with $m = n = 12$, $d_s = d_t = 7$, $\alpha = 1.7$.

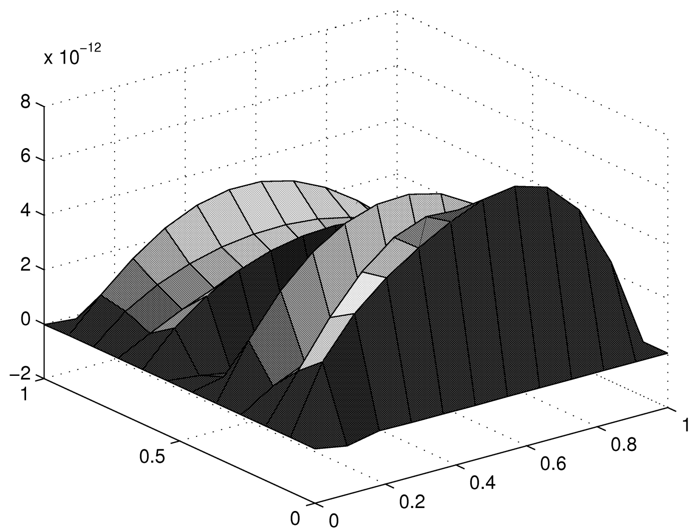

Figure 10. Errors of RBCM with $m = n = 12$, $d_s = d_t = 7$, $\alpha = 1.9$.

5. Conclusions

One dimensional SFRDE is studied by RBCM, in order to get the higher accuracy, the fractional term is transformed into Riemman integral by fractional integration. The time variable and spatial variable are solved by RBCM at the same time, matrix equation of SFRDE can be obtained which is same as the SFRDE. While for the two dimensional SFRDE and non-linear SFRDE, the LRBCM can also be used to get the corresponding matrix equation.

Acknowledgements

The work of Jin Li was supported by Natural Science Foundation of Shandong Province (Grant No. ZR2022MA003).

The authors would also like to thank the referees for their constructive comments and remarks which helped improve the quality of the paper.

Conflict of interest

The author declare that they have no conflict of interest.

References

1. M. Abramowitz, I. A. Stegun, *Handbook of mathematical functions with formulas, graphs, and mathematical tables*, US Government Printing Office, 1948
2. F. Dell'Accio, F. Di Tommaso, G. Ala, E. Francomano, Electric scalar potential estimations for non-invasive brain activity detection through multinode Shepard method, *2022 IEEE 21st Mediterranean Electrotechnical Conference*, 2022. https://doi.org/10.1109/MELECON53508.2022.9842881
3. I. T. Huseynov, A. Ahmadova, A. Fernandez, N. I. Mahmudov, Explicit analytical solutions of incommensurate fractional differential equation systems, *Appl. Math. Comput.*, **390** (2021), 125590. https://doi.10.1016/j.amc.2020.125590
4. T. Jiang, X. Wang, J. Ren, J. Huang, J. Yuan, A high-efficient accurate coupled mesh-free scheme for 2D/3D space-fractional convection-diffusion/Burgersi problems, *Comput. Math. Appl.*, 2022, https://doi.org/10.1016/j.camwa.2022.10.020
5. Y. Chen, Q. Li, H. Yi, Y. Huang, Immersed finite element method for time fractional diffusion problems with discontinuous coefficients, *Comput. Math. Appl.*, **128** (2022), 121–129 https://doi.10.1016/j.camwa.2022.09.023
6. N. Srivastava, V. K. Singh, L3 approximation of Caputo derivative and its application to time-fractional wave equation, *Math. Comput. Simul.*, **205** (2023), 532–557 https://doi.10.1016/j.matcom.2022.10.003
7. W. Bu, S. Shu, X. Yue, A. Xiao, W. Zeng, Space-time finite element method for the multi-term time-space fractional diffusion equation on a two-dimensional domain, *Comput. Math. Appl.*, **78** (2019), 1367–1379 https://doi.10.1016/j.camwa.2018.11.033

8. S. Toprakseven, A weak Galerkin finite element method on temporal graded meshes for the multi-term time fractional diffusion equations, *Comput. Math. Appl.*, **128** (2022), 108–120 https://doi.10.1016/j.camwa.2022.10.012
9. A. Ghafoor, N. Khan, M. Hussain, R. Ullah, A hybrid collocation method for the computational study of multi-term time fractional partial differential equations, *Comput. Math. Appl.*, **128** (2022), 130–144 https://doi.10.1016/j.camwa.2022.10.005
10. P. Berrut, M. S. Floater, G. Klein, Convergence rates of derivatives of a family of barycentric rational interpolants. *Appl. Numer. Math.*, **61**, (2011), 989–1000. https://doi.10.1016/j.apnum.2011.05.001
11. J. P. Berrut, S. A Hosseini, G. Klein, The linear barycentric rational quadrature method for Volterra integral equations, *SIAM J. Sci. Comput.*, **36**, (2014), 105–123. https://doi.10.1137/120904020
12. M. S. Floater, K. Hormann, Barycentric rational interpolation with no poles and high rates of approximation, *Numer. Math.*, **107** (2007), 315–331. https://doi.org/10.1007/s00211-007-0093-y
13. G. Klein, J. Berrut, Linear rational finite differences from derivatives of barycentric rational interpolants, *SIAM J. Numer. Anal.*, **50** (2012), 643–656. https://doi.org/10.1137/110827156
14. G. Klein, J. Berrut, Linear barycentric rational quadrature, *BIT Numer. Math.*, **52** (2012), 407–424. https://doi.org/10.1007/s10543-011-0357-x
15. R. Baltensperger, J. P. Berrut, The linear rational collocation method, *J. Comput. Appl. Math.*, **134** (2001), 243–258. https://doi.org/10.1016/S0377-0427(00)00552-5
16. J. Li, Y. Cheng, Linear barycentric rational collocation method for solving heat conduction equation, *Numer. Methods Partial Differ. Equations*, **37** (2021), 533–545. https://doi.org/10.1002/num.22539
17. J. Li, Y. Cheng, Linear barycentric rational collocation method for solving second-order Volterra integro-differential equation, *Comput. Appl. Math.*, **39** (2020), 92. https://doi.org/10.1007/s40314-020-1114-z
18. J. Li, Y. Cheng, Barycentric rational method for solving biharmonic equation by depression of order, *Numer. Methods Partial Differ. Equations*, **37** (2021), 1993–2007. https://doi.org/10.1002/num.22638
19. J. Li, Linear barycentric rational collocation method for solving biharmonic equation, *Demonstr. Math.*, **55** (2022), 587–603. https://doi.org/10.1515/dema-2022-0151
20. J. Li, X. Su, K. Zhao, Barycentric interpolation collocation algorithm to solve fractional differential equations, *Math. Comput. Simul.*, **205** (2023), 340–367. https://doi.org/10.1016/j.matcom.2022.10.005
21. Z. Q. Wang, S. P. Li, *Barycentric interpolation collocation method for nonlinear problems*, National Defense Industry Press, 2015.
22. Z. Q. Wang, Z. K. Xu, J. Li, Mixed barycentric interpolation collocation method of displacement-pressure for incompressible plane elastic problems, *Chin. J. Appl. Mech.*, **35** (2018), 195–201.
23. Z. Wang, L. Zhang, Z. Xu, J. Li, Barycentric interpolation collocation method based on mixed displacement-stress formulation for solving plane elastic problems, *Chin. J. Appl. Mech.*, **35** (2018), 304–309. https://doi.org/10.11776/cjam.35.02.D002

24. F. Dell'Accio, F. Di Tommaso, O. Nouisser, N. Siar, Solving Poisson equation with Dirichlet conditions through multinode shepard operators, *Comput. Math. Appl.*, **98** (2021), 254–260. https://doi.org/10.1016/j.camwa.2021.07.021

25. W. H. Luo, T. Z. Huang, X. M. Gu, Y. Liu, Barycentric rational collocation methods for a class of nonlinear parabolic partial differential equations, *Appl. Math. Lett.*, **68** (2017), 13–19. https://doi.org/10.1016/j.aml.2016.12.011

26. F. Delli'Accio, F. Di Tommaso, Rate of convergence of multinode shepard operators, *Dolomit. Res. Notes Approx.*, **12** (2019), 1–6. https://doi.org/10.14658/pupj-drna-2019-1-1

27. T. J. Rivlin, *Chebyshev polynomials*, Courier Dover Publications, 2020.

28. K. Jing, N. Kang, A convergent family of bivariate Floater-Hormann rational interpolants, *Comput. Methods Funct. Theory*, **21** (2021), 271–296. https://doi.org/10.1007/s40315-020-00334-9